



Published in final edited form as:

*Circ Res.* 2023 April 28; 132(9): 1127–1140. doi:10.1161/CIRCRESAHA.122.321693.

## Evidence that Binding of Cyclic GMP to the Extracellular Domain of Na<sup>+</sup>/K<sup>+</sup>-ATPase Mediates Natriuresis

Brandon A. Kemp, BA,

Nancy L. Howell, BA,

John J. Gildea, PhD,

Josh D. Hinkle, PhD,

Jeffrey Shabanowitz, PhD,

Donald F. Hunt, PhD,

Mark R. Conaway, PhD,

Susanna R. Keller, MD,

Robert M. Carey, MD

Department of Medicine-Division of Endocrinology and Metabolism (BAK, NLH, SRK, RMC), the Department of Pathology (JJG) the Department of Chemistry (JDH, JS, DFH) and the Division of Translational Research and Applied Statistics, Department of Public Health Sciences (MRC), University of Virginia, Charlottesville, VA

### Abstract

**Background:** Extracellular renal interstitial (RI) cyclic guanosine 3'5'-monophosphate (cGMP) inhibits renal proximal tubule (RPT) sodium (Na<sup>+</sup>) reabsorption via Src family kinase activation. Through which target extracellular cGMP acts to induce natriuresis is unknown. We hypothesized that cGMP binds to the extracellular  $\alpha$ 1-subunit of Na<sup>+</sup>/K<sup>+</sup>-ATPase (NKA) on RPT basolateral membranes to inhibit Na<sup>+</sup> transport similar to ouabain, a cardiotonic steroid.

**Methods and Results:** Urine Na<sup>+</sup> excretion was measured in uninephrectomized 12-week-old female Sprague-Dawley rats that received RI infusions of vehicle (D<sub>5</sub>W), cGMP (18, 36, and 72  $\mu$ g/kg/min; 30 min each), or cGMP + rostafuroxin (12 ng/kg/min) or were subjected to pressure natriuresis +/- rostafuroxin infusion. Rostafuroxin is a digitoxigenin derivative that displaces ouabain from NKA. RI cGMP and raised renal perfusion pressure induced natriuresis and increased phosphorylated Src<sup>Tyr416</sup> and Erk 1/2<sup>Thr202/Tyr204</sup>; these responses were abolished with rostafuroxin co-infusion. To assess cGMP binding to NKA, we performed competitive binding

---

Correspondence: Dr. Robert M. Carey, P.O. Box 801414, University of Virginia Health System, Charlottesville, VA 22908-1414; telephone: 434-924-5510; fax 434-982-3626; rmc4c@virginia.edu.

Disclosures:

None

Supplemental Materials

Expanded Materials and Methods

Online Figures S1–S10

Online Table S1

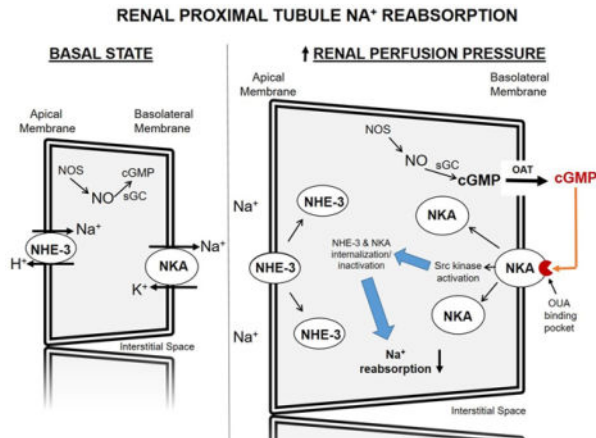
Data Set

References 25–32

studies with isolated rat RPTs using bodipy-ouabain (2  $\mu\text{M}$ ) + cGMP (10  $\mu\text{M}$ ) or rostavuroxin (10  $\mu\text{M}$ ) and 8-Biotin-11-cGMP (2  $\mu\text{M}$ ) + ouabain (10  $\mu\text{M}$ ) or rostavuroxin (10  $\mu\text{M}$ ). cGMP or rostavuroxin reduced bodipy-ouabain fluorescence intensity, and ouabain or rostavuroxin reduced 8-Biotin-11-cGMP staining. We crosslinked isolated rat RPTs with 4-N<sub>3</sub>-PET-8-Biotin-11-cGMP (azido-BIO-cGMP; 2  $\mu\text{M}$ ); 8-N<sub>3</sub>-6-Biotin-10-cAMP (azido-BIO-cAMP) served as negative control. Precipitation with streptavidin beads followed by immunoblot analysis showed that RPTs after crosslinking with azido-BIO-cGMP exhibited a significantly stronger signal for NKA than non-crosslinked samples and crosslinked or non-crosslinked azido-BIO-cAMP RPTs. Ouabain (10  $\mu\text{M}$ ) reduced NKA in crosslinked azido-BIO-cGMP RPTs confirming fluorescence staining. Azido-BIO-cGMP crosslinked samples were separated by SDS gel electrophoresis and slices corresponding to NKA molecular weight excised and processed for mass spectrometry. NKA was the second most abundant protein with 50 unique NKA peptides covering 47% of amino acids in NKA. Molecular modeling demonstrated a potential cGMP docking site in the ouabain binding pocket of NKA.

**Conclusions:** cGMP can bind to NKA and thereby mediate natriuresis.

## Graphical Abstract



Schematic diagram of cyclic GMP-dependent signaling pathways in the renal proximal tubule cell leading to reduced sodium (Na<sup>+</sup>) transport and natriuresis in response to increased renal perfusion pressure. Increased renal perfusion pressure increases cGMP production in renal proximal tubule cells. In a unidirectional process, cGMP is transported across the basolateral membrane by a probenecid-sensitive organic anion transporter into the renal interstitial fluid where it binds to the ouabain binding pocket on the extracellular domain of NKA. cGMP binding to NKA activates Src kinase resulting in internalization and inactivation of Na<sup>+</sup> transporters, NHE-3 and NKA, and natriuresis. cGMP, cyclic 3',5'-guanosine monophosphate; NHE-3, sodium-hydrogen exchanger-3; NKA, sodium-potassium-ATPase; NO, nitric oxide; NOS, soluble nitric oxide synthase; OAT, organic anion transporter; OUA, ouabain; sGC, soluble guanylyl cyclase; Src, Src-family kinase.

## Keywords

Natriuresis; Sodium-Potassium ATPase; Receptor; Cyclic GMP; Pressure-Natriuresis; Ouabain; Rostafuroxin

**Subject Terms:**High Blood Pressure

---

**INTRODUCTION**

Pressure-natriuresis is a major homeostatic mechanism wherein an acute rise in arterial blood pressure (BP) induces a rapid increase in renal sodium ( $\text{Na}^+$ ) excretion.<sup>1</sup> This leads to a decrease in extracellular fluid volume preventing a long term rise in BP. Virtually all forms of hypertension (experimental and human) are characterized by impaired natriuretic responses to increased BP. Normal  $\text{Na}^+$  excretion in the hypertensive state is achieved at the expense of increased BP.<sup>1</sup> The mechanism underlying pressure-natriuresis at high renal perfusion pressure is unknown. While manipulations of several endocrine and/or paracrine systems shift the pressure-natriuresis curve to the right (less sensitive) or left (more sensitive), they do not abolish the natriuretic response to increased pressure.<sup>2-5</sup>

Guanosine cyclic 3',5'-monophosphate (cGMP) is natriuretic.<sup>6,7</sup> It is generated in renal proximal tubule cells (RPTC) by nitric oxide (NO) action on RPTC soluble guanylyl cyclase (sGC).<sup>8-13</sup> Following its biosynthesis, cGMP is exported out of the RPTC into the extracellular renal interstitial (RI) space by a probenecid-sensitive organic anion transporter.<sup>14-16</sup> Endogenous extracellular RI cGMP inhibits RPTC  $\text{Na}^+$  uptake and induces natriuresis.<sup>6,15</sup> Because increased renal perfusion pressure increases RI cGMP production and natriuresis, both of which are abolished by intrarenal sGC inhibition, RI cGMP has been considered a candidate mediator of pressure-natriuresis.<sup>7,17-19</sup>

The cellular mechanisms through which extracellular RI cGMP regulates natriuresis and pressure-natriuresis are unknown. A large quantity of the cyclic nucleotide is exported from RPTCs into the RI compartment within minutes after administration of an NO donor or increased renal perfusion pressure.<sup>6,7,17-19</sup> cGMP extrusion is non-saturable, and is unidirectional because extracellular cGMP does not re-enter the RPTC.<sup>16,20</sup> Therefore, we hypothesized that RI cGMP binds to an RPTC basolateral membrane molecule that transmits the signal for inhibition of  $\text{Na}^+$  transport.

A potential receptor for cGMP in the renal epithelial cell basolateral membrane is  $\text{Na}^+/\text{K}^+$ -ATPase (NKA). While NKA is well recognized as an ion pump, NKA also has been identified as a new class of plasma membrane receptors linked to the Src family kinase signaling pathway.<sup>21</sup> NKA is a heterodimer consisting of a catalytic  $\alpha$ -subunit and a  $\beta$ -subunit required for insertion into the plasma membrane. NKA normally maintains Src in an inactivated state. Exposure to low concentrations of cardiotonic steroids (e.g. ouabain, marinobufagenin, and digoxin) that bind to the extracellular domain of the NKA  $\alpha$ -subunit, stimulates release and phosphorylation of Src kinase.<sup>21</sup> Activation of this pathway in the basolateral membranes of renal epithelial cells induces internalization and inactivation of NKA and reduces the expression and activity of  $\text{Na}^+/\text{H}^+$  exchanger-3 (NHE-3), thereby reducing  $\text{Na}^+$  reabsorption.<sup>22,23</sup>

Our previous studies showed that both exogenous cGMP and increased renal perfusion pressure resulting in increased endogenous RI cGMP, induce natriuresis in a Src-dependent manner, demonstrating that Src is an important downstream signaling molecule for extracellular cGMP-induced natriuresis.<sup>24</sup> Here we show evidence that cGMP can bind to the extracellular domain of NKA and thereby activate the Src kinase signaling pathway to induce natriuresis.

## MATERIALS AND METHODS

### Data Availability.

The data that support the findings of this study are available from the corresponding author upon reasonable request.

Please see the Online Data Supplement for detailed methods [confocal microscopy, total RPTC membrane preparation and Western blot analysis, renal proximal tubule (RPT) isolation and experimentation, cross-linking and immunoprecipitation experiments, mass spectrometry (MS) preparation and analysis, Na<sup>+</sup> efflux assay<sup>25</sup>, molecular modeling<sup>26–29</sup>, human NKA ATPase activity<sup>30,31</sup> and power calculations<sup>32</sup>]. All experimental protocols were approved by the Animal Care and Use Committee at the University of Virginia and performed in accordance with the National Institutes of Health Guide for the Care and Use of Laboratory Animals.

### Animal Preparation:

The experiments were conducted with 12-week-old female and male Sprague–Dawley rats (Envigo) housed in a vivarium under controlled conditions (temperature 21±1°C; humidity 60±10%; light 8:00–20:00) and fed a normal Na<sup>+</sup> diet (0.30% Na<sup>+</sup>).

On the day of experimentation, rats were anesthetized with inactin (100 mg/kg body weight) [Protocol 1] or ketamine (60 mg/kg) and xylazine (4 mg/kg) [Protocol 2, 4 and 5] and a tracheostomy was performed using polyethylene tubing (PE-240) to assist respiration. Direct cannulation of the right internal jugular vein using PE-10 tubing provided intravenous access through which 4% bovine serum albumin (BSA) in 5% dextrose in water (D<sub>5</sub>W) was infused at 40 µL/min. Direct cannulation of the right carotid artery with PE-50 tubing provided arterial access for monitoring mean arterial pressure (MAP). Following a midline laparotomy, the right kidney was removed (so that substances infused directly into the left kidney would not spill over to the opposite kidney confounding the results), and the ureter of the remaining left kidney was cannulated (PE-10) to collect urine for the measurement of urine Na<sup>+</sup> excretion (U<sub>NaV</sub>). For Protocols 4–5, normal rats were anesthetized with ketamine (60 mg/kg) and xylazine (4 mg/kg) and kidneys were removed for competitive binding studies.

### Renal Cortical Interstitial Infusion:

An open bore micro-infusion catheter (PE-10) was inserted under the renal capsule into the cortex of the left kidney to ensure the renal interstitial (RI) infusion of vehicle D<sub>5</sub>W or pharmacological agent at 2.5 µL/min with a syringe pump (Harvard; model 55–222). When

two agents were infused, separate catheters were employed. Vetbond tissue adhesive (3M Animal Care Products) was used to secure the catheter(s) and prevent interstitial pressure loss in the kidney.

#### **BP Measurements:**

MAP was measured by the direct intra-carotid method with the use of a digital BP analyzer (Micromed, Inc). MAP was recorded every 5 min and averaged for all periods. Experiments were initiated at the same time each day to avoid diurnal variation in BP.

#### **Pressure-Natriuresis (P-N) Model:**

We used a variant of the P-N model of Roman and Cowley that has been previously used in our laboratory.<sup>7</sup> Renal perfusion pressure was increased during the experimental period by tying off the infrarenal aorta and clamping the superior mesenteric artery.

#### **Pharmacological Agents:**

Pharmacological agents and their biochemical structures are shown in Figure S1. Cyclic guanosine 3'5'-monophosphate (cGMP; 18, 36, and 72  $\mu\text{g}/\text{kg}/\text{min}$  for acute studies and 0.5, 1.0, and 10  $\mu\text{M}$  for competitive binding studies; BioLog; Cat. #G001). 8-Biotin-11-cGMP (BIO-cGMP; 2  $\mu\text{M}$  for competitive binding studies; Biolog; Cat. #B025-01). 4-N<sub>3</sub>-PET-8-Biotin-11-cGMP (azido-BIO-cGMP; 2  $\mu\text{M}$  for crosslinking studies and competitive binding studies; Biolog; Cat. #A186). 8-Biotin-11-cAMP (BIO-cAMP; 2  $\mu\text{M}$  for competitive binding studies; Biolog; Cat. #B03-01). 8-N<sub>3</sub>-6-Biotin-10-cAMP (azido-BIO-cAMP; 2  $\mu\text{M}$  for cross-linking studies; Biolog; Cat. #A127-001). Rostafuroxin; 12 ng/kg/min for non-pressure-natriuresis experiments; 2.4 and 12 ng/kg/min for pressure-natriuresis experiments; and 0.5, 1.0, and 10  $\mu\text{M}$  for competitive binding studies; courtesy of Dr. Patrizia Ferrari. Ouabain (0.5, 1.0, and 10  $\mu\text{M}$  for competitive binding studies; Sigma; Cat. #03125). BODIPY (dipyrrromethene boron difluoride)-ouabain (2  $\mu\text{M}$ ) for competitive binding studies (Invitrogen Molecular Probes; Cat. #B23461).

#### **Statistical Analysis:**

Data are presented as mean  $\pm$  1 SE. For all data sets, the repeated measures analysis was performed with an unstructured covariance matrix in SAS PROC MIXED program. The ANOVA with permutation P value was based on 2000 or 10,000 permutations of group assignment to individual N values and a repeated measures analysis with an unstructured covariance matrix. The method of permutation preserves the within-animal correlation structure and does not rely on the assumption of normality in the data. The permutation procedure was chosen because the power of nonparametric tests in small sample sizes is generally low and there are few quality options for nonparametric repeated measures analyses.<sup>35</sup> Only within-test corrections were performed and there was no experiment-wide multiple test correction. P values  $<0.05$  were considered statistically significant with the maximum significance reported by the software as  $P < 0.001$ . Values that were greater than 2 standard deviations above or below the mean were also excluded which resulted in removing 6 rats from U<sub>Na</sub>V analyses and 3 cross-linking values from competitive binding studies. Representative Western blot images were chosen based upon which of the 2 blots most

closely represented the quantitative data. All blots used for analysis are included in the Online Data Supplement. For *in vivo* studies, each experimental condition was performed on the same day alongside a control and completely randomized by a coin flip. Western blot and Na<sup>+</sup> efflux studies were not blinded. For confocal competitive binding studies, the experiments were blinded and completely randomized by a coin flip. Proximal tubules were first selected using DAPI autofluorescence and then imaged for streptavidin Alexa Fluor 488 staining.

### Specific Protocols:

**(1) Effects of Intrarenal cGMP infusion ± Intrarenal Infusion of Ouabain Antagonist Rostafuroxin on U<sub>Na</sub>V, MAP, pSrc<sup>Tyr416</sup>, Src, pErk 1/2<sup>Thr202/Tyr204</sup>, and Erk 1/2, Protein Levels.**—Following a 1h equilibration period, the following groups of female and male rats were studied: (1) Female Control (N=8): rats received RI infusions of vehicle D<sub>5</sub>W for the entire 2h study. (2) Female cGMP (N=14): rats received RI infusion of vehicle for 30 min during the control period followed by cumulative RI infusions of cGMP (18, 36, and 72 µg/kg/min; each dose for 30 min) during the experimental periods. (3) Male cGMP (N=5): rats received RI infusion of vehicle for 30 min during the control period followed by cumulative RI infusions of cGMP (18, 36, and 72 µg/kg/min; each dose for 30 min) during the experimental periods. (4) Female cGMP + rostafuroxin (N=7): rats received RI infusion of vehicle for 30 min during the control period followed by the RI co-infusion of cGMP (18, 36, and 72 µg/kg/min; each dose for 30 min) + rostafuroxin (12 ng/kg/min) during the experimental periods. U<sub>Na</sub>V and MAP were measured for each period. At the end of the experiment, kidneys were harvested for Western blot analysis (N=6 for each condition).

In a second set of experiments, following a 1h equilibration period, the following groups of female rats were studied. (1) Control (N=6): rats received RI infusion of vehicle for 2h. (2) cGMP (N=7): rats received RI infusion of cGMP (72 µg/kg/min) for 2h. (3) cGMP + rostafuroxin (N=10): rats received RI infusion of cGMP (72 µg/kg/min) + rostafuroxin (12 ng/kg/min) for 2h. (4) Rostafuroxin (N=7): rats received RI infusion of rostafuroxin (12 ng/kg/min) for 2h. U<sub>Na</sub>V and MAP were measured for each period.

**(2) Effects of Increased Renal Perfusion Pressure ± Intrarenal Infusion of Ouabain Antagonist Rostafuroxin on U<sub>Na</sub>V, MAP, pSrc<sup>Tyr416</sup>, Src, pErk 1/2<sup>Thr202/Tyr204</sup>, and Erk 1/2, Protein Levels.**—Following a 1h equilibration period, the following groups of female rats were studied: (1) Control (N=6): rats received RI infusion of vehicle D<sub>5</sub>W for two 30 min periods. (2) P-N Control (N=14): rats received RI infusion of vehicle D<sub>5</sub>W during both the 30 min control and 30 min high renal perfusion pressure periods. (3) P-N + Rostafuroxin 2.4 (N=8): rats received RI infusion of rostafuroxin (2.4 ng/kg/min) during both the control and high renal perfusion pressure periods. (4) P-N + Rostafuroxin 12 (N=7): rats received RI infusion of rostafuroxin (12 ng/kg/min) during both the control and high renal perfusion pressure periods. U<sub>Na</sub>V and MAP were measured for each period. At the end of the experiment, kidneys were harvested for control, P-N Control, and P-N + Rostafuroxin (12 ng/kg/min) and processed for Western blot analysis (N=6 for each condition).

**(3) Na<sup>+</sup> Efflux Assay.**—Male Wistar-Kyoto rat RPTCs were treated as follows for 20 min and underwent Na<sup>+</sup> efflux measurements (N=6 wells for each condition and 20 measurements taken from each well). (1) Control: PBS. (2) Fenoldopam: 1 μM. (3) cGMP: 2 μM. (4) Azido-BIO-cGMP: 2 μM.

**(4) Competitive Binding Confocal Microscopy Experiments.**—RPTs were isolated from normal female Sprague-Dawley rat kidneys (N=4 kidneys for each protocol **A-F**) and experiments for all conditions were performed in triplicate in a 96-well plate.

- A. Effects of cGMP on BODIPY-Ouabain Binding:** (1) Control: Opti-MEM. (2) BODIPY-ouabain: 2 μM. (3) BODIPY-ouabain + cGMP: BODIPY-ouabain (2 μM) + cGMP (0.5, 1.0, and 10 μM).
- B. Effects of Ouabain on BIO-cGMP Binding:** (1) Control: Opti-MEM. (2) BIO-cGMP: 2 μM. (3) BIO-cGMP + Ouabain: BIO-cGMP (2 μM) + ouabain (10 μM).
- C. Effects of RF on BODIPY-Ouabain Binding:** (1) Control: Opti-MEM. (2) BODIPY-ouabain: 2 μM. (3) BODIPY-ouabain + rostafuroxin: BODIPY-ouabain (2 μM) + rostafuroxin (0.5, 1.0, and 10 μM).
- D. Effects of Rostafuroxin on BIO-cGMP Binding:** (1) Control: Opti-MEM. (2) BIO-cGMP: 2 μM. (3) BIO-cGMP + Rostafuroxin: BIO-cGMP (2 μM) + rostafuroxin (10 μM).
- E. BIO-cAMP Binding:** (1) Control: Opti-MEM. (2) BIO-cAMP: 2 μM.
- F. Effects of cGMP on Azido-BIO-cGMP Binding:** (1) Control: Opti-MEM. (2) Azido-BIO-cGMP: 2 μM. (3) Azido-BIO-cGMP + cGMP: azido-BIO-cGMP (2 μM) + cGMP (10 μM).

**(5) Azido Cyclic Nucleotide Cross-linking Experiments.**—RPTs were isolated from normal female Sprague-Dawley rat kidneys (N=4 kidneys for each protocol **A-C**) and experiments for all conditions were performed in triplicate in a 96-well plate.

- A. Cross-linking of Azido-BIO-cGMP to RPTs and αNKA Protein (N=3):** (1) Control: Opti-MEM. (2) Azido-BIO-cGMP crosslinked: 2 μM. (3) Azido-BIO-cGMP non-crosslinked: 2 μM.
- B. Cross-linking of Azido-BIO-cGMP and Azido-BIO-cAMP to αNKA (N=8):** (1) Azido-BIO-cGMP cross-linked: 2 μM. (2) Azido-BIO-cGMP non-cross-linked: 2 μM. (3) Azido-BIO-cAMP cross-linked: 2 μM. (4) Azido-BIO-cAMP non-cross-linked: 2 μM.
- C. Effects of Ouabain on Cross-linking of Azido-BIO-cGMP to αNKA (N=6):** (1) Azido-BIO-cGMP cross-linked: 2 μM. (2) Azido-BIO-cGMP non-cross-linked: 2 μM. (3) Azido-BIO-cGMP cross-linked + Ouabain: Azido-BIO-cGMP (2 μM) + ouabain (10 μM). (4) Azido-BIO-cGMP non-cross-linked + Ouabain: Azido-BIO-cGMP (2 μM) + ouabain (10 μM).

**(6) Identification of  $\alpha$ NKA Peptide Sequences with Mass Spectrometry in RPTs Cross-linked to Azido-BIO-cGMP.**—Three kidney samples processed following azido-BIO-cGMP cross-linking in **Protocol 5** were subjected to cross-linking and mass spectrometry as described in the Online Data Supplement.

## RESULTS

### Effects of Intrarenal cGMP infusion $\pm$ Intrarenal Infusion of Ouabain Antagonist Rostafuroxin on $U_{NaV}$ and MAP:

cGMP and ouabain are both natriuretic. To test whether cGMP, similar to ouabain, mediates natriuresis by binding to NKA, we used rostafuroxin, a digitoxigenin derivative that displaces ouabain from NKA and thereby inhibits its action.<sup>33,34</sup> Confirming previous results<sup>6</sup>, we found that progressively increasing RI infusion rates of cGMP (18, 36, and 72  $\mu$ g/kg/min) in volume-expanded rats engendered a stepwise significant increase in  $U_{NaV}$  (30 min collection periods;  $P < 0.001$  for all 3 experimental doses; Figure 1, Panel A). However, the cGMP-induced increase in  $U_{NaV}$  was abolished by RI co-infusion of rostafuroxin (12 ng/kg/min) during all cGMP infusion periods ( $P = 0.007$ ,  $P = 0.002$ , and  $P = 0.003$ , respectively). Neither cGMP nor rostafuroxin induced any significant changes in MAP during the experiment (Figure S2, **Panel A**). In a separate set of experiments in volume expanded rats, RI cGMP infusion (72  $\mu$ g/kg/min) increased  $U_{NaV}$  progressively during 2 consecutive 60 min collection periods (Figure S3, **Panel A**;  $P = 0.002$  and  $P < 0.001$ , respectively). The cGMP-induced natriuresis during both collection periods was abolished by RI co-infusion of rostafuroxin (12 ng/kg/min;  $P < 0.001$  for both), while rostafuroxin alone had no effect on  $U_{NaV}$  and was not different from vehicle control. There were no changes in MAP during any of these experiments (Figure S3, **Panel B**). There was no significant difference in the natriuretic response to cGMP between male and female rats (Figure S4).

### Effects of Increased Renal Perfusion Pressure on $U_{NaV}$ in the Presence or Absence of Intrarenal Infusion of Rostafuroxin:

cGMP mediates the natriuretic effect of pressure natriuresis.<sup>7</sup> If this is mediated through binding to the ouabain binding site in NKA, we would expect inhibition of the effect with rostafuroxin. As shown in volume expanded rats during 2 consecutive 30 min collection periods (Figure 1, Panel B), increasing MAP (and consequently renal perfusion pressure) during the second collection period (Figure S2, **Panel B**;  $P < 0.001$ ) resulted in a highly significant natriuretic response (Figure 1, Panel B;  $P < 0.001$ ). RI infusion of rostafuroxin at 2.4 ng/kg/min partially inhibited the pressure natriuretic response (Figure 1, Panel B;  $P = 0.034$ ), while increasing the infusion rate to 12 ng/kg/min abolished pressure-natriuresis ( $P < 0.001$ ). All rats experienced a similar significant rise in MAP during the high renal perfusion pressure period (Figure S2, **Panel B**).

### Effects of Intrarenal cGMP infusion and of Increased Renal Perfusion Pressure in the Presence or Absence of Intrarenal Infusion of Ouabain Antagonist Rostafuroxin on pSrc<sup>Tyr416</sup>, Src, pErk1/2<sup>Thr202/Tyr204</sup>, and Erk 1/2 Protein Levels:

cGMP and ouabain both induce natriuresis through Src kinase activation.<sup>24</sup> Consistent with our earlier observations, RI cGMP infusion (18, 36, and 72  $\mu$ g/kg/min) as well as increased



renal perfusion pressure significantly increased Src<sup>Tyr416</sup> phosphorylation in total kidney cortical homogenates in volume expanded rats (Figure 2, Panel A; P<0.001 and Figure S5, **Panel A**; P<0.001, respectively) without changing total Src (Panels B), thus increasing the ratio of pSrc<sup>Tyr416</sup> / Src (Figure 2, Panel C; P=0.001 and Figure S5, **Panel C**; P=0.002, respectively). cGMP- and increased renal perfusion pressure-induced Src phosphorylation was inhibited by rostavuroxin infusion (12 ng/kg/min) [Figure 2, Panel A; P=0.007 and Figure S5, **Panel A**; P<0.001, respectively] thus also decreasing the ratio (Figure 2, Panel C; P=0.017 and Figure S5, **Panel C**; P<0.001, respectively). RI cGMP infusion and increased renal perfusion pressure also significantly increased Erk 1/2 phosphorylation (Figure 2, Panel D; P<0.001 and Figure S5, **Panel D**; P<0.001, respectively), without changing total Erk 1/2 (Panels E), thus increasing the ratio of pErk<sup>Thr202/Tyr204</sup> / total Erk 1/2 (Figure 2, Panel F; P=0.001 and Figure S5, **Panel F**; P=0.001, respectively). cGMP- and pressure-induced Erk phosphorylation and ratio were similarly inhibited by rostavuroxin (Figures 2 and S5, **Panels D** and **F**; P<0.001 and P=0.002, and P<0.001 and P=0.001, respectively).

### Na<sup>+</sup> Efflux Assay

To determine whether cGMP could inhibit NKA activity, we performed a Na<sup>+</sup> efflux assay in WKY rat RPTCs *in vitro* with assay conditions configured so that changes in Na<sup>+</sup> efflux in RPTCs could be attributed to NKA activity (Figure 3, Panel A). Fenoldopam is a dopamine 1-like receptor agonist that inhibits Na<sup>+</sup> reabsorption via inactivation of NKA. In this assay, RPTCs treated with fenoldopam (1 μM), demonstrated 33.6 ± 4.4% inhibition of basal Na<sup>+</sup> efflux (P<0.001) and served as the positive control. RPTCs treated with either cGMP (2 μM) or the analog azido-BIO-cGMP (2 μM) [used below for crosslinking studies], resulted in similar reductions in Na<sup>+</sup> efflux (36.7 ± 6.7% (P<0.001) and 33.1 ± 7% (P=0.001) respectively). These findings demonstrate that cGMP can inhibit NKA activity in RPTCs and that azido-BIO-cGMP is a biologically active analog of cGMP.

We also determined the dose response relationship between cGMP and Na<sup>+</sup> efflux in WKY rat RPTCs. cGMP inhibited Na<sup>+</sup> efflux in a concentration-dependent manner (Figure S6) with an IC<sub>50</sub> value of 36 nM cGMP. This is close to physiological extracellular cGMP concentrations in the interstitial fluid of the kidney cortex where we previously measured cGMP levels in the low nM range.<sup>16</sup>

### Competitive Binding Studies

To determine whether azido-BIO-cGMP or cGMP could bind to NKA in freshly isolated rat RPTs, we conducted a series of competitive binding studies using fluorescence microscopy (Figures 3–5). Figure 3, Panel B demonstrates a significantly strong fluorescence signal above background for azido-BIO-cGMP (2 μM; P<0.001) that was abolished in the presence of 10 μM cGMP (P<0.001). These results suggest that azido-BIO-cGMP and cGMP are competing for the same binding site on RPTs. Figure 4, Panel A demonstrates a strong fluorescence signal above background for BODIPY-ouabain in RPTs under control conditions (P<0.001) and a progressive reduction in signal after addition of increasing cGMP concentrations (0.5, 1.0, and 10 μM). The BODIPY-ouabain signal is significantly abolished with 1.0 μM and 10 μM cGMP (P=0.037 and P<0.001, respectively). To demonstrate the reverse, strong BIO-cGMP binding to RPTs (Panel B; P<0.001) is

significantly reduced by 10  $\mu$ M ouabain (Panel B;  $P=0.018$ ). Figure 5, Panel A demonstrates that significant BODIPY-ouabain fluorescence signal above background in RPTs ( $P=0.001$ ) is also reduced by rostafuroxin at 1.0  $\mu$ M and 10  $\mu$ M ( $P=0.026$  and  $P<0.001$ , respectively). Panel B indicates that the significant BIO-cGMP signal in RPTCs ( $P=0.001$ ) can in turn also be inhibited by 10  $\mu$ M rostafuroxin ( $P=0.006$ ). As a negative control, Figure S7 demonstrates that BIO-cAMP does not bind to RPTs as no fluorescence signal over background is detectable.

### Cross-linking Studies:

Building upon the competitive binding studies, we next performed cross-linking studies (Figure 6) to determine whether cGMP indeed binds to the extracellular domain of NKA in normal rat RPTCs. Panel A demonstrates that in freshly isolated RPTs, azido-BIO-cGMP cross-linked samples (2  $\mu$ M) adsorbed to streptavidin beads exhibit a strong signal for NKA by Western blot, while RPTs that received either vehicle (Opti-MEM) or azido-BIO cGMP without cross-linking resulted in little to no signal for NKA. Panel B confirmed that RPTs with cross-linked azido-BIO-cGMP exhibited a strong signal for NKA that was significantly weaker for non-cross-linked azido-BIO-cGMP ( $42.5 \pm 6.3\%$ ;  $P<0.001$ ) and cross-linked ( $46.8 \pm 5.1\%$ ;  $P<0.001$ ) or non-cross-linked Azido-BIO-cAMP samples (2  $\mu$ M) [ $39.9 \pm 4.6\%$ ;  $P<0.001$ ]. In Panel C, we demonstrate that when ouabain (10  $\mu$ M) is present during cross-linking the amount of NKA is reduced in cross-linked Azido-BIO-cGMP RPTs ( $P<0.001$ ) confirming competitive binding studies using fluorescence microscopy.

### Mass Spectrometry (MS) Results:

Azido-BIO-cGMP crosslinked samples ( $N=3$ ) were separated in a Tris-HCl gel and stained with Coomassie SimplyBlue SafeStain. A gel slice corresponding to the molecular size of NKA (110 kDa) was excised and processed for mass spectrometry. Figure 7 displays the peptide National Center for Biotechnology Information (NCBI) sequence for *Rattus Norvegicus* NKA. The underlined text indicates tryptic peptides identified by mass spectrometry when searched against the NCBI *Rattus Norvegicus* NKA reference sequence using Byonic by Protein Metrics. The double underline indicates that some of the peptides identified were truncated versions of that peptide. Peptides were accepted with a false recovery rate of 1%. The mass spectrometry analysis identified 47 unique peptides in the sample and demonstrated a 46.1% sequence coverage (472/1023 residues) of NKA. Figure S8 displays the most abundant proteins identified in the gel slice by mass spectrometry.

### In Silico Docking of cGMP to NKA:

Three potential docking sites were identified using AutoDock Vina and a grid box centered around the ouabain binding site. The highest scoring site is located between TM2, TM8 and the L9–10 loop (Figure 8, tan colored cGMP). The second is overlapping the ouabain binding site and the lowest scoring site is found at the FXYD- $\beta$ -subunit interface (Figure 8, teal and orange colored cGMP, respectively).

### NKA ATPase Assay:

We measured ATPase activity of purified human NKA in the presence of varying concentrations of cGMP (Figure S9). Addition of <10  $\mu$ M cGMP to the assay medium did not significantly affect ATPase activity, while 1 mM cGMP reduced ATPase activity by ~30%.

## DISCUSSION

Our analysis provides strong evidence that cGMP competes with ouabain to bind to the extracellular domain of NKA, thereby transducing its natriuretic response in a Src- and Erk-dependent manner. (1) The increase in  $U_{NaV}$  elicited by RI infusion of cGMP and pressure-natriuresis was abolished by the ouabain antagonist rostafuroxin; (2) the cGMP-induced increase in RPTC Src and Erk phosphorylation was also abolished by rostafuroxin; (3) in freshly isolated RPTs, cGMP inhibited ouabain competitive binding and *vice-versa*, and both cGMP and ouabain binding was displaced by rostafuroxin; (4) after crosslinking, azido-BIO-cGMP was associated with NKA as demonstrated by Western blot analysis, and the NKA signal was reduced with ouabain; (5) tandem mass spectrometry analysis of the gel slice corresponding to NKA in azido-cGMP crosslinked samples contained a large number of NKA peptides covering 46.1% of the amino acid sequence of NKA; and *in silico* studies demonstrating a potential docking site for cGMP in the ouabain binding pocket of NKA.

NKA is well-established as an ion pump, transporting 3  $Na^+$  ions out and two  $K^+$  ions into cells at the expense of a single ATP molecule. This active energy-dependent ion transport process creates a cellular diffusion gradient for several other membrane transporters that regulate fluid and electrolyte balance and the absorption of nutrients, such as amino acids and glucose.<sup>36</sup> Indeed, NKA-induced ion transport is requisite for eukaryotic cell survival. However, accumulating evidence now suggests that, independently of its critical role as an ion transporter, NKA can also serve as a receptor transducing downstream signaling events, thereby affecting multiple cellular functions.<sup>21,37-41</sup> To activate the NKA signaling pathway, most studies have employed the cardiotonic steroid ouabain, a specific NKA ligand that binds to the extracellular domain of all NKA  $\alpha$ -subunit isoforms.<sup>37,38</sup> Although saturating concentrations of ouabain completely inhibit NKA transport capacity, sub-saturating concentrations, while having little or no effect on intracellular  $Na^+$  concentration, activate a variety of signaling molecules.<sup>21,42</sup> Thus, NKA has a dual role as ion transporter and receptor transducing downstream cell signaling events.

An important example is the  $\alpha_1$ NKA/Src complex that serves as a receptor for cardiotonic steroids and other NKA ligands to activate protein/lipid kinase cascades to generate reactive oxygen species and stimulate  $Ca^{++}$  oscillations in a cell-specific manner.<sup>21,42</sup> Src-family kinases are membrane-associated non-receptor tyrosine kinases and NKA regulates Src activity through a phosphorylation-dependent mechanism.<sup>43</sup> Binding of cardiotonic steroids to the NKA/Src receptor complex leads to activation of Src and initiation of a signal transduction process.<sup>42</sup> Studies from our laboratory have shown that Src is an important downstream signaling molecule for extracellular cGMP- and pressure-induced natriuresis.<sup>24</sup> In those studies, we demonstrated that both cGMP and increased renal perfusion pressure induce natriuresis in a Src-dependent manner and that

Src phosphorylation is independent of reactive oxygen or nitrogen species generation during pressure-natriuresis.<sup>24</sup> During pressure-natriuresis, cGMP is transported out of RPTC cells by a probenecid-sensitive organic anion transporter into the RI compartment and does not re-enter cells.<sup>44</sup> Thus, cGMP serves as an extracellular modulator of pressure-natriuresis, the molecular mechanisms of which are summarized in the **Graphical Abstract**. The results of the current study clarify the target for extracellular cGMP to mediate pressure-natriuresis. We demonstrate that cGMP binds to NKA using photo-affinity labeling followed by tandem mass spectrometry.

Photo-affinity labeling is a well-recognized method to investigate ligand-protein interactions and has previously been employed to detect cyclic nucleotide binding proteins.<sup>45,46</sup> Photo-affinity tags function by causing a short-lived reactive species following activation by a specific wavelength of light. In the case of the azide tag used in our experiments, excitation by 254 nm UV light generates both a nitrene and dihydroazepine species, both of which can react with primary amines present within proteins. Proteins with high affinity for the chemical tag (in this case cGMP) are likely to be in close proximity to the tag following photoactivation and are thus likely to bind to the reactive species while other proteins are unlikely to react nonspecifically due to the reactive species being quenched by solution. This allows for selective tagging of high-affinity proteins that can be purified by an affinity tag present on the reagent, in this case biotin.

A significant advantage offered by mass spectrometry analysis over immunoassays is the high degree of confidence in the protein's identity. The peptides identified in our analysis successfully identified NKA within the excised gel band with a high degree of confidence; nearly half of the  $\alpha$ NKA amino acid sequence could be mapped to  $\alpha$ NKA-specific peptide sequences observed within the analysis. We were unsuccessful in identifying a specific peptide bound to azido-BIO-cGMP. This result is not surprising in light of incomplete sequence coverage that often results from bottom-up protein sequencing experiments, particularly when using gel band digestion strategies.<sup>47,48</sup> Failure to directly identify cGMP bound peptides may also be due, at least in part, to hydrophobic transmembrane domains being dramatically underrepresented in tryptic digests of membrane resident proteins.<sup>49</sup>

The fact that ouabain inhibits cGMP binding to NKA and *vice versa* suggested the possibility that cGMP binds to the same binding pocket as ouabain in NKA. Indeed molecular docking validated potential binding of extracellular cGMP to NKA with one of the docking models overlapping with the ouabain binding pocket, thereby potentially explaining the observed displacement of ouabain by cGMP.<sup>50</sup> However, docking does not allow estimation of affinity.<sup>51,52</sup> The observation that cGMP inhibits ATPase activity of purified NKA only at supraphysiological concentrations makes it unlikely that the effects of cGMP on  $\text{Na}^+$  reabsorption result from direct ATPase inhibition. However, dopamine and other hormones reduce  $\text{Na}^+$  flux in renal proximal tubule cells indirectly by NKA internalization.<sup>53–55</sup> Thus, concentrations without a detectable effect on ATPase activity can still have biological effects. As described above, cGMP as well as ouabain have been linked to Src-kinase signaling. Although the details remain to be determined, non-inhibiting concentrations of endogenous glycosides can regulate intracellular  $\text{Ca}^{++}$  concentration and kinase activation, thereby affecting numerous signaling pathways.<sup>56</sup> It should thus be

considered that cGMP acts similarly, through NKA or via an independent receptor, to initiate a cascade leading to NKA internalization (as summarized in the **Graphical Abstract**). Although our data strongly suggest binding of cGMP directly to NKA, and molecular modeling suggests that cGMP interaction with the ouabain binding pocket is possible, we lack direct evidence that binding of cGMP to this site mediates natriuresis. It is still possible that binding of cGMP to another, currently unknown, ouabain binding site on a NKA-associated protein mediates the effect. Future research will address this.

## Supplementary Material

Refer to Web version on PubMed Central for supplementary material.

## Acknowledgements:

We thank Drs. Poul Nissen and Michael Habeck (Aarhus University, Aarhus, Denmark) for performing the *in silico* studies and ATPase inhibition studies with cGMP. Special thanks to Protein Metrics for providing Bionic.

## Sources of Funding:

The data reported in this manuscript were supported by NIH grants 2-R01-HL-128173 (Robert M. Carey, PI) and GM-037537 (Donald F. Hunt, PI).

## LIST OF ABBREVIATIONS

<b>ATP</b>	adenosine triphosphate
<b>BIO</b>	biotin
<b>BP</b>	blood pressure
<b>cAMP</b>	cyclic AMP
<b>cGMP</b>	cyclic GMP
<b>ERK 1/2</b>	extracellular signal-regulated protein kinase 1/2
<b>K<sup>+</sup></b>	potassium
<b>MAP</b>	mean arterial pressure
<b>Na<sup>+</sup></b>	sodium
<b>NCBI</b>	National Center for Biotechnology Information
<b>NHE-3</b>	sodium-hydrogen exchanger-3
<b>NKA</b>	sodium-potassium ATPase
<b>NO</b>	nitric oxide
<b>pERK</b>	phosphorylated ERK
<b>P-N</b>	pressure natriuresis
<b>pSrc</b>	phosphorylated Src

<b>RI</b>	renal interstitial
<b>RPT</b>	renal proximal tubule
<b>RPTC</b>	renal proximal tubule cell
<b>sGC</b>	soluble guanylyl cyclase
<b>Src</b>	Src family kinase
<b>U<sub>Na</sub>V</b>	urinary sodium excretion

## REFERENCES

- Guyton AC, Coleman TG, Young DB, Lohmeier TE, DeClue JW. Salt balance and long-term blood pressure control. *Annu Rev Med.* 1980;31:15–27. [PubMed: 6994602]
- Gross V, Lippoldt A, Schneider W, Luft FC. Effect of captopril and angiotensin II receptor blockade on pressure natriuresis in transgenic TGR (mRen-2)27 rats. *Hypertension.* 1995;26:471–479. [PubMed: 7649584]
- Gross JM, Dwyer JE, Knox FG. Natriuretic response to increased pressure is preserved with COX-2 inhibitors. *Hypertension.* 1999;34:1163–1167. [PubMed: 10567199]
- Tornel J, Madred MI, Garcia-Salom M, Wirth KJ, Fenoy FJ. Role of kinins in the control of renal papillary blood flow, pressure-natriuresis and arterial pressure. *Circ Res.* 2000;86:589–595. [PubMed: 10720421]
- Ivy JR, Bailey MA. Pressure natriuresis and the renal control of arterial blood pressure. *J Physiol.* 2014;592:3955–3967. [PubMed: 25107929]
- Jin XH, Siragy HM, Carey RM. Renal interstitial cGMP mediates natriuresis by direct tubule mechanism. *Hypertension.* 2001;38:309–316. [PubMed: 11566896]
- Jin XH, McGrath HE, Gildea JJ, Siragy HM, Felder RA, Carey RM. Renal interstitial guanosine cyclic 3',5'-monophosphate mediates pressure natriuresis via protein kinase G. *Hypertension.* 2004;43:1133–1139. [PubMed: 15007031]
- Ujiie K, Yuen J, Hogarth L, Danziger R, Star RA. Localization and regulation of endothelial NO synthase mRNA expression in rat kidney. *Am J Physiol.* 1994;267:F296–F302. [PubMed: 7520668]
- Terada Y, Tomita K, Nonoguchi H, Marumo F. Polymerase chain reaction localization of constitutive nitric oxide synthase and soluble guanylyl cyclase messenger RNAs in microdissected rat nephron segments. *J Clin Invest.* 1992;90:659–665. [PubMed: 1379616]
- Eitle E, Hiranyachattada S, Wang H, Harris PJ. Inhibition of proximal tubular fluid absorption by nitric oxide and atrial natriuretic peptide in rat kidney. *Am J Physiol.* 1998;274:C1075–C1080. [PubMed: 9575805]
- Guzman NJ, Fang MZ, Tang SS, Ingelfinger JR, Garg LC. Autocrine inhibition of Na<sup>+</sup>/K<sup>+</sup>-ATPase by nitric oxide in mouse proximal tubule epithelial cells. *J Clin Invest.* 1995;95:2083–2088. [PubMed: 7537754]
- Roczniak A, Burns KD. Nitric oxide stimulates guanylyl cyclase and regulates sodium transport in rabbit proximal tubule. *Am J Physiol.* 1996;270:F106–F115. [PubMed: 8769828]
- Wang T Nitric oxide regulates HCO<sup>3</sup> and Na<sup>+</sup> transport by a cGMP-mediated mechanism in the kidney proximal tubule. *Am J Physiol.* 1997;272:F242–F248. [PubMed: 9124402]
- Chevalier RL, Fern RJ, Garmey M, ElDahr SS, Gomez RA, Devente J. Localization of cGMP after infusion of ANP or nitroprusside in the maturing rat. *Am J Physiol Renal Physiol.* 1992;262:F417–F427.
- Chevalier RL, Fang GD, Garmey M. Extracellular cGMP inhibits transepithelial sodium transport by LLC-PK1 renal tubule cells. *Am J Physiol.* 1996;270:F283–F288. [PubMed: 8779888]
- Sasaki S, Siragy HM, Gildea JJ, Felder RA, Carey RM. Production and role of extracellular guanosine cyclic 3',5'-monophosphate in sodium uptake in human proximal tubule cells. *Hypertension.* 2004;43:286–291. [PubMed: 14718358]

17. Ahmed F, Kemp BA, Howell NL, Siragy HM, Carey RM. Extracellular renal guanosine cyclic 3',5'-monophosphate modulates nitric oxide- and pressure-induced natriuresis. *Hypertension*. 2007;50:958–963. [PubMed: 17846351]
18. Park J, Kemp BA, Howell NL, Gildea JJ, Keller SR, Carey RM. Intact microtubules are required for natriuretic responses to nitric oxide and increased renal perfusion pressure. *Hypertension*. 2008;51[part 2]:494–499. [PubMed: 18172053]
19. Lieb DC, Kemp BA, Howell NL, Gildea JJ, Carey RM. Reinforcing feedback loop of renal cyclic guanosine 3',5'-monophosphate and interstitial hydrostatic pressure in pressure-natriuresis. *Hypertension*. 2009;54:1278–1283. [PubMed: 19841292]
20. Hamet P, Pang SC, Tremblay J. Atrial natriuretic factor-induced egression of cyclic guanosine 3',5'-monophosphate in cultured vascular smooth muscle and endothelial cells. *J Biol Chem*. 1989;264:12364–12369. [PubMed: 2545708]
21. Aperia A, Akkuratov EE, Fontana JM, Brismar H. Na<sup>+</sup>-K<sup>+</sup>-ATPase, a new class of plasma membrane receptors. *Am J Physiol Cell Physiol*. 2016;310:C491–C495. [PubMed: 26791490]
22. Oweis S, Wu L, Kiels PR, Zhao H, Mulhotra D, Gishan PK, Xie Z, Shapiro JL, Liu J. Cardiac glycoside downregulates NHE3 activity and expression in LLC-PK1 cells. *Am J Physiol Renal Physiol*. 2006;290:F997–F1008. [PubMed: 16352745]
23. Cai H, Wu L, Qu W, Malhotra D, Xie Z, Shapiro JI, Liu J. Regulation of apical NHE3 trafficking by ouabain-induced activation of the basolateral Na<sup>+</sup>-K<sup>+</sup>-ATPase receptor complex. *Am J Physiol Cell Physiol*. 2008;294:C555–C563. [PubMed: 18077602]
24. Nascimento NRF, Kemp BA, Howell NL, Gildea JJ, Santos CF, Harris TE, Carey RM. Role of Src family kinase in extracellular renal cyclic guanosine 3',5'-monophosphate- and pressure-induced natriuresis. *Hypertension*. 2011;58:107–113. [PubMed: 21482955]
25. Woost PG, Orosz DE, Jin W, Jacobberger JW, Douglas JG, Hopfer U. Immortalization and characterization of proximal tubule cells derived from kidneys of spontaneously hypertensive and normotensive rats. *Kidney Int*. 1996;50:125–134. [PubMed: 8807581]
26. Laursen M, Yatime L, Nissen P, Fedosova NU. Crystal structure of the high-affinity Na<sup>+</sup>,K<sup>+</sup>-ATPase-ouabain complex with Mg<sup>2+</sup> bound in the cation binding site. *Proceedings of the National Academy of Sciences*. 2013; 110, 10958–10963.
27. Morris GM et al. AutoDock4 and AutoDockTools4: Automated docking with selective receptor flexibility. *J Comput Chem*. 2009;30, 2785–2791. [PubMed: 19399780]
28. Trott O, Olson AJ. AutoDock Vina: improving the speed and accuracy of docking with a new scoring function, efficient optimization, and multithreading. *J Comput Chem*. 2010;31:455–461. [PubMed: 19499576]
29. Pettersen EF et al. UCSF ChimeraX: Structure visualization for researchers, educators, and developers. *Protein Sci*. 2021;30:70–82 (2021). [PubMed: 32881101]
30. Habeck M, Kapri-Pardes E, Sharon M, Karlish SJD. Specific phospholipid binding to Na,K-ATPase at two distinct sites. *Proceedings of the National Academy of Sciences USA*. 2017;114, 2904–2909.
31. Baginski ES, Foa PP, Zak, B. Determination of phosphate: Study of labile organic phosphate interference. *Clinica Chimica Acta*. 1967;15, 155–158.
32. Faul F, Erdfelder E, Buchner A, Lang AG. Statistical power analysis using G\*Power 3.1: Tests for correlation and regression analysis. *Behav Res Methods*. 2009;41:1149–1160.
33. Ferrari P, Ferrandi M, Valentini G, Bianchi G. Rostafuroxin: an ouabain antagonist that corrects renal and vascular Na<sup>+</sup>-K<sup>+</sup>-ATPase alterations in ouabain and adducin-dependent hypertension. *A J P Regul Integr Comp Physiol* 2006;290:R529–35.
34. Ferrari P Rostafuroxin: an ouabain-inhibitor counteracting specific forms of hypertension. *Biochim Biophys Acta (BBA)—Molecular Basis of Disease*. 2010;1802:1254–8. [PubMed: 20083196]
35. Good P “Permutation, Parametric and Bootstrap Tests of Hypotheses, 3rd edition”. *Springer Series in Statistics* 2005. ISBN: 978-1-44-1907-6.
36. Na Blanco G.,K-ATPase subunit heterogeneity as a mechanism for tissue-specific ion regulation. *Semin Nephrol*. 2005;25:292–303. [PubMed: 16139684]
37. Lingrel JB, The physiological significance of cardiotonic steroid/ouabain binding site of the Na,K-ATPase. *Annu Rev Physiol*. 2010;72:395–412. [PubMed: 20148682]

38. Pierre SV, Xie Z. The Na,K ATPase receptor complex: its organization and membership. *Cell Biochem Biophys.* 2006;46:303–316. [PubMed: 17272855]
39. Tian J, Cai T, Yuan Z, Wang H, Liu L, Haas M, Maksimova E, Huang XY, Xie ZJ. Binding of Crc to Na<sup>+</sup>-K<sup>+</sup>-ATPase forms a functional signaling complex. *Mol Biol Cell.* 2006;17:317–326. [PubMed: 16267270]
40. Reinhard L, Tidlow H, Clausen MJ, Nissen P. Na<sup>+</sup>,K<sup>+</sup>-ATPase as a docking station: protein-protein complexes of the Na<sup>+</sup>,K<sup>+</sup>-ATPase. *Cell Mol Life Sci.*2013;70:205–222. [PubMed: 22695678]
41. Xie JX, Li X, Xie Z. Regulation of renal function and structure by the signaling Na/KATPase. *IUBMB Life.* 2013;65:991–998. [PubMed: 24323927]
42. Cui X, Xie Z. Protein interaction and Na/K-ATPase-mediated signal transduction. *Molecules.* 2017.22:990; doi:10.3390/molecules22060990. [PubMed: 28613263]
43. Thomas SM, Brugge JS. Cellular functions regulated by Src family kinases. *Annu Rev Cell Dev Biol.* 1997;13:317–326.
44. Sasaki S, Siragy HM, Gildea JJ, Felder RA, Carey RM. Production and role of extracellular guanosine cyclic 3',5'-monophosphate in sodium uptake in human proximal tubule cells. *Hypertension.* 2004;43:286–291. [PubMed: 14718358]
45. Smith E, Collins I. Photoaffinity labeling in target- and binding-site identification. *Future Med Chem.* 2015;7:159–183. [PubMed: 25686004]
46. Friedman DL, Chambers DA. Cyclic nucleotide binding proteins detected by photoaffinity labeling in nucleus and cytoplasm of bovine liver. *Proc Nat Acad Sci USA.* 1978;75:5286–5290. [PubMed: 214781]
47. Weber PJ, Beck-Sickinger AG. Comparison of the photochemical behavior of four different photo-activatable probes. *J Peptide Res.* 1997;49:375–383. [PubMed: 9211218]
48. Smith E, Collins I. Photoaffinity labeling in target- and binding-site identification. *Future Med Chem.* 2015;7:159–183. [PubMed: 25686004]
49. Lee HC, Carroll A, Crossett B, Connolly A, Batarseh A, Djordjevic MA. Improving the identification and coverage of plant transmembrane proteins in *Medicago* using bottom-up proteomics. *Front Plant Sci.* 2020;11:595726. doi: 10.3389/fpls.2020.595726.eCollection 2020. [PubMed: 33391307]
50. Laursen M, Yatime L, Nissen P, Fedosova NU. Crystal structure of the high affinity Na<sup>+</sup>, K<sup>+</sup>-ATPase-ouabain complex with Mg<sup>2+</sup> bound in the cation binding site. *Proc Natl Acad Sci USA.* 2013;110:10958–10963. [PubMed: 23776223]
51. Meli R, Morris GM, Biggin PC. Scoring Functions for Protein-Ligand Binding Affinity Prediction using Structure-Based Deep Learning: A Review. *Front Bioinform.*2022:2.
52. Pantsar T, Poso A. Binding Affinity via Docking: Fact and Fiction. *Molecules.* 2018;23.
53. Yudowski GA, Efendies R, Pedemonte CH, Katz AI, Berggren P-O. Phosphoinositide-3 kinase binds to a proline-rich motif in the Na<sup>+</sup>,K<sup>+</sup>-ATPase  $\alpha$  subunit and regulates its trafficking. *Proc Nat Acad Sci USA.* 2000;97:6556–6561. [PubMed: 10823893]
54. Efendiev R, Das-Panja K, Cinelli AR, Bertorello AM, Pedemonte GH. Localization of intracellular compartments that exchange Na,K-ATPase molecules with the plasma membrane in a hormone-dependent manner. *Br J Pharmacol.* 2007;151:1006–1013. [PubMed: 17533417]
55. Gildea JJ, Isreal JA, Johnson AK, Zhang J, Jose PA, Felder RA. Caveolin-1 and dopamine-mediated internalization of NaKATPase in human renal proximal tubule cells. *Hypertension.* 2009;54:1070–1076. [PubMed: 19752292]
56. Blaustein MP & Hamlyn JM Ouabain, endogenous ouabain and ouabain-like factors: The Na(+)-pump/ouabain receptor, its linkage to NCX, and its myriad functions. *Cell Calcium* 86, 102159 (2020). [PubMed: 31986323]



## Novelty and Significance

### What is known?

- Pressure-natriuresis is a major homeostatic mechanism wherein an acute rise in blood pressure induces a rapid increase in renal sodium ( $\text{Na}^+$ ) excretion.
- Extracellular renal interstitial cyclic guanosine 3'5'-monophosphate (cGMP) inhibits renal proximal tubule (RPT)  $\text{Na}^+$  reabsorption, induces natriuresis and is a candidate mediator of pressure-natriuresis.
- The molecular target by which extracellular cGMP acts to induce natriuresis is unknown.

### What new information does this article contribute?

- The cardiotonic steroid ouabain inhibits cGMP binding to sodium-potassium-ATPase (NKA) and *vice versa*, suggesting that cGMP binds to the same binding pocket as ouabain in NKA.
- The cGMP- and pressure-natriuresis-induced increases in RPT Src and ERK phosphorylation and  $\text{Na}^+$  excretion are abolished by the ouabain antagonist rostauroxin.
- After crosslinking, azido-BIO-cGMP is associated with NKA, protein analysis of the gel slice encompassing the cross-linked NKA contains a large number of NKA peptides, and *in silico* studies demonstrate a potential docking site for cGMP in the ouabain binding pocket of NKA.

### Summary

Extracellular renal interstitial cGMP inhibits RPT Na<sup>+</sup> reabsorption via Src family kinase activation, but the target by which cGMP acts to induce natriuresis is unknown. We hypothesized that cGMP binds to the extracellular  $\alpha 1$ -subunit of NKA on RPT basolateral membranes to inhibit Na<sup>+</sup> transport similar to ouabain. RI cGMP and raised renal perfusion pressure induced natriuresis and increased phosphorylated Src<sup>Tyr416</sup> and Erk 1/2<sup>Thr202/Tyr204</sup>; these responses were abolished by rostafuroxin, which displaces ouabain from NKA. To assess cGMP binding to NKA, we performed competitive binding studies: cGMP or rostafuroxin reduced bodipy-ouabain fluorescence intensity, and ouabain or rostafuroxin reduced 8-Biotin-11-cGMP staining. RPTs after cross-linking with azido-BIO-cGMP and precipitation with streptavidin beads exhibited a significantly stronger signal for NKA than non-cross-linked samples. Ouabain reduced NKA in cross-linked azido-BIO-cGMP RPTs confirming fluorescence staining. Azido-BIO-cGMP cross-linked samples were processed for mass spectrometry and 50 unique NKA peptides covering 47% of the sequence of NKA were identified. Molecular modeling demonstrated a potential cGMP docking site in the ouabain-binding pocket of NKA. These studies provide evidence that cGMP can bind to the extracellular domain of NKA and may thereby transduce its natriuretic response in a Src- and Erk-dependent manner.

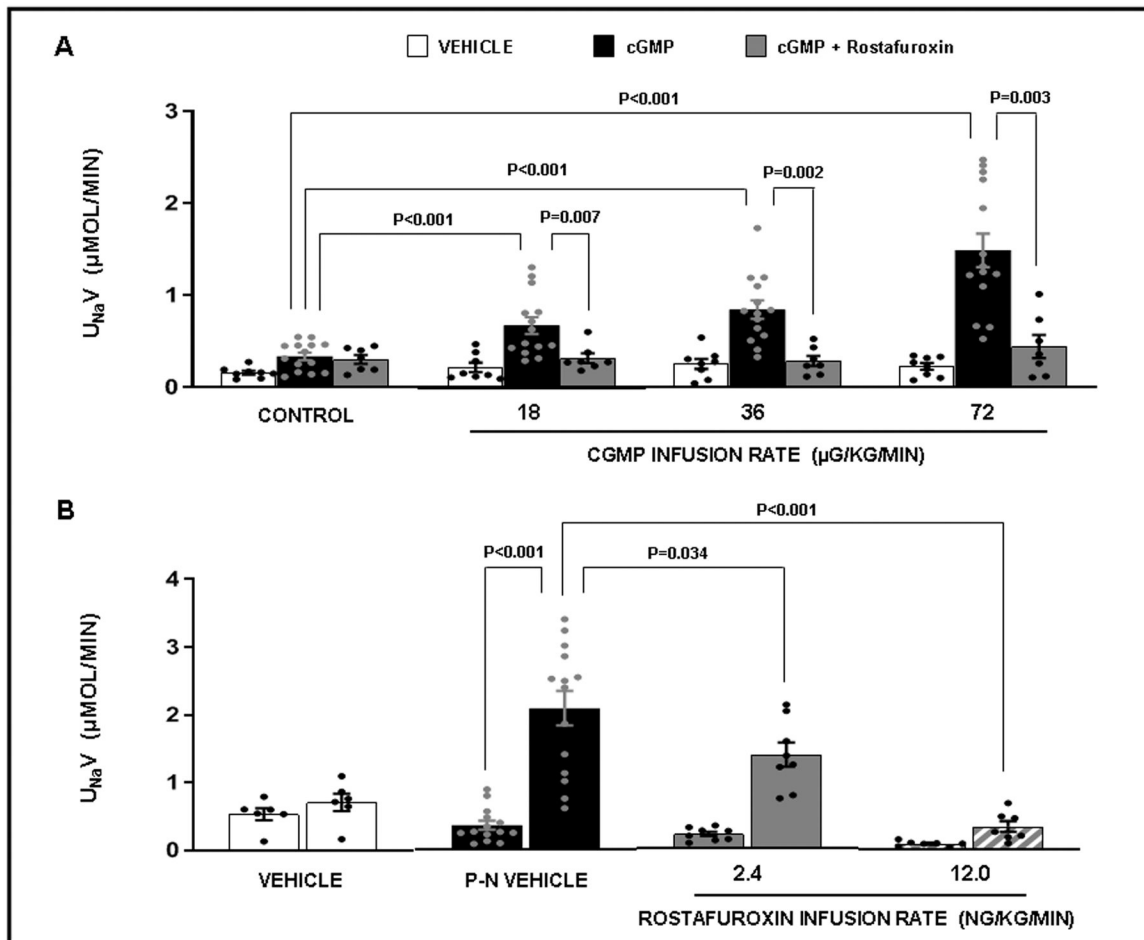


**Figure 1.**

**Panel A.** Urine sodium ( $\text{Na}^+$ ) excretion ( $U_{\text{Na}}V$ ) in response to the following conditions: (□) Time Control (N=8): rats received renal interstitial (RI) infusion of vehicle (VEH)  $\text{D}_5\text{W}$  for the entire 2h study. (■) cGMP (N=14): rats received RI infusion of VEH for 30 min during the control period followed by cumulative RI infusions of cGMP (18, 36, and 72  $\mu\text{g}/\text{kg}/\text{min}$ ; each dose for 30 min) during the experimental periods. (▣) cGMP + Rostafuroxin (RF) (N=7): rats received RI infusion of VEH for 30 min during the control period followed by the RI co-infusion of cGMP + RF (12  $\text{ng}/\text{kg}/\text{min}$ ) during the experimental periods. Results are reported as  $\mu\text{mol}/\text{min}$ . **Panel B.** Urine sodium ( $\text{Na}^+$ ) excretion ( $U_{\text{Na}}V$ ) in response to the following conditions: (□) Vehicle (VEH) Control (N=6): rats received renal interstitial (RI) infusion of VEH  $\text{D}_5\text{W}$  during both 30 min periods. (■) Pressure-natriuresis (P-N) VEH (N=14): rats received RI infusion of VEH during both the 30 min control and 30 min high renal perfusion pressure periods. (▣) P-N + Rostafuroxin (RF; 2.4  $\text{ng}/\text{kg}/\text{min}$ ) (N=8): rats received RI infusion of RF during both the 30 min control and 30 min high renal perfusion pressure periods. (▤) P-N + RF (12  $\text{ng}/\text{kg}/\text{min}$ ) (N=7): rats received RI infusion of RF during both the 30 min control and high renal perfusion pressure periods. Results are reported as  $\mu\text{mol}/\text{min}$ . Statistical significance was determined by using the repeated measures analysis with an unstructured covariance matrix in SAS PROC MIXED program. The ANOVA with

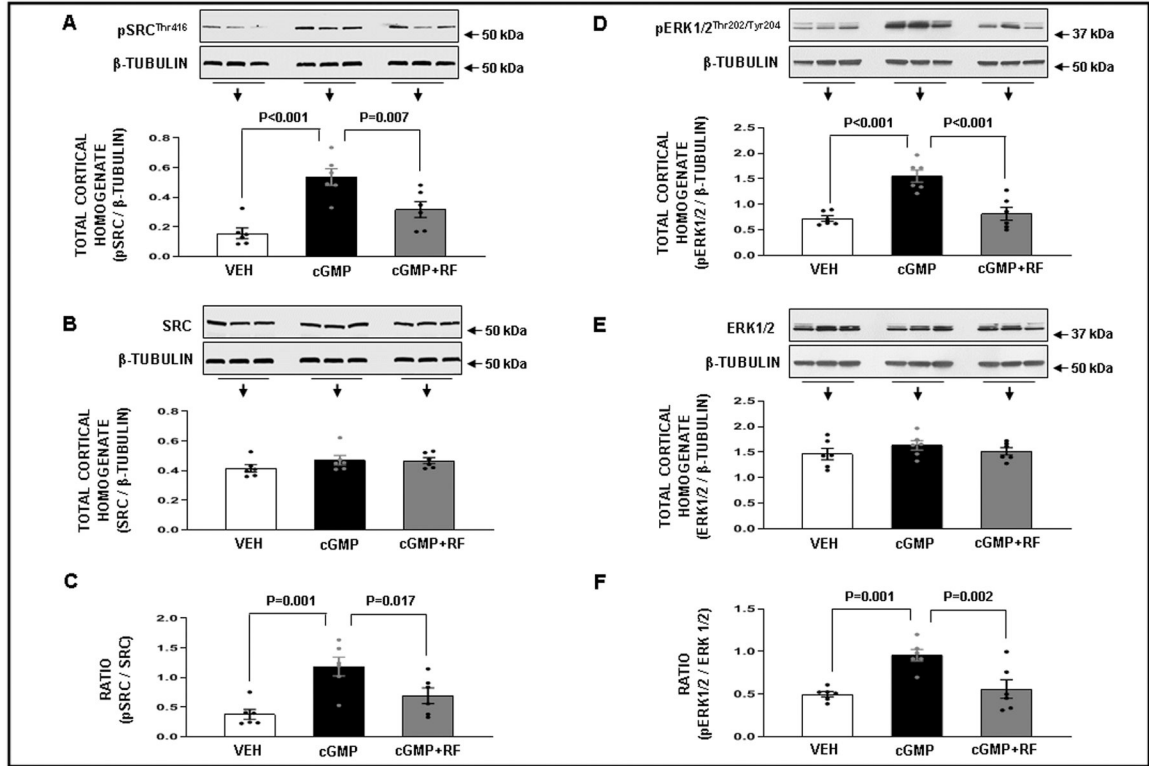
permutation P value was based on 2000 permutations of group assignment to individual N values and a repeated measures analysis with an unstructured covariance matrix.

Author Manuscript

Author Manuscript

Author Manuscript

Author Manuscript

**Figure 2.**

**Panel A.** Western blot analysis of total cortical homogenate phospho-Src<sup>Thr416</sup> (pSrc<sup>Thr416</sup>) protein levels in response to the following conditions: (□) Time Control Vehicle (VEH; N=6): rats received renal interstitial (RI) infusion of VEH D<sub>5</sub>W for 2h. (■) cGMP (N=6): rats received RI infusion of VEH for 30 min during the control period followed by cumulative RI infusions of cGMP (18, 36, and 72  $\mu$ g/kg/min; each dose for 30 min) during the experimental periods. (▨) cGMP + Rostafuroxin (RF) (N=6): rats received RI infusion of VEH for 30 min during the control period followed by the RI co-infusion of cGMP + RF (12 ng/kg/min) during the experimental periods. **Panel B.** Western blot analysis of total Src protein levels in response to the conditions in **Panel A**. **Panel C.** Ratio of (pSrc<sup>Thr416</sup> /  $\beta$ -Tubulin) / (total Src /  $\beta$ -Tubulin) in response to the conditions in **Panel A**. **Panel D.** Western blot analysis of phospho- Erk1/2<sup>Thr202/Tyr204</sup> (pErk 1/2<sup>Thr202/Tyr204</sup>) protein levels in response to the conditions in **Panel A**. **Panel E.** Western blot analysis of total Erk protein levels in response to the conditions in **Panel A**. **Panel F.** Ratio of (pErk 1/2<sup>Thr202/Tyr204</sup> /  $\beta$ -Tubulin) / (total Erk 1/2 /  $\beta$ -Tubulin) in response to the conditions in **Panel A**. Data represent mean  $\pm$  1 SE. Statistical significance was determined by using the repeated measures analysis with an unstructured covariance matrix in SAS PROC MIXED program. The ANOVA with permutation P value was based on 10,000 permutations of group assignment to individual N values and a repeated measures analysis with an unstructured covariance matrix.

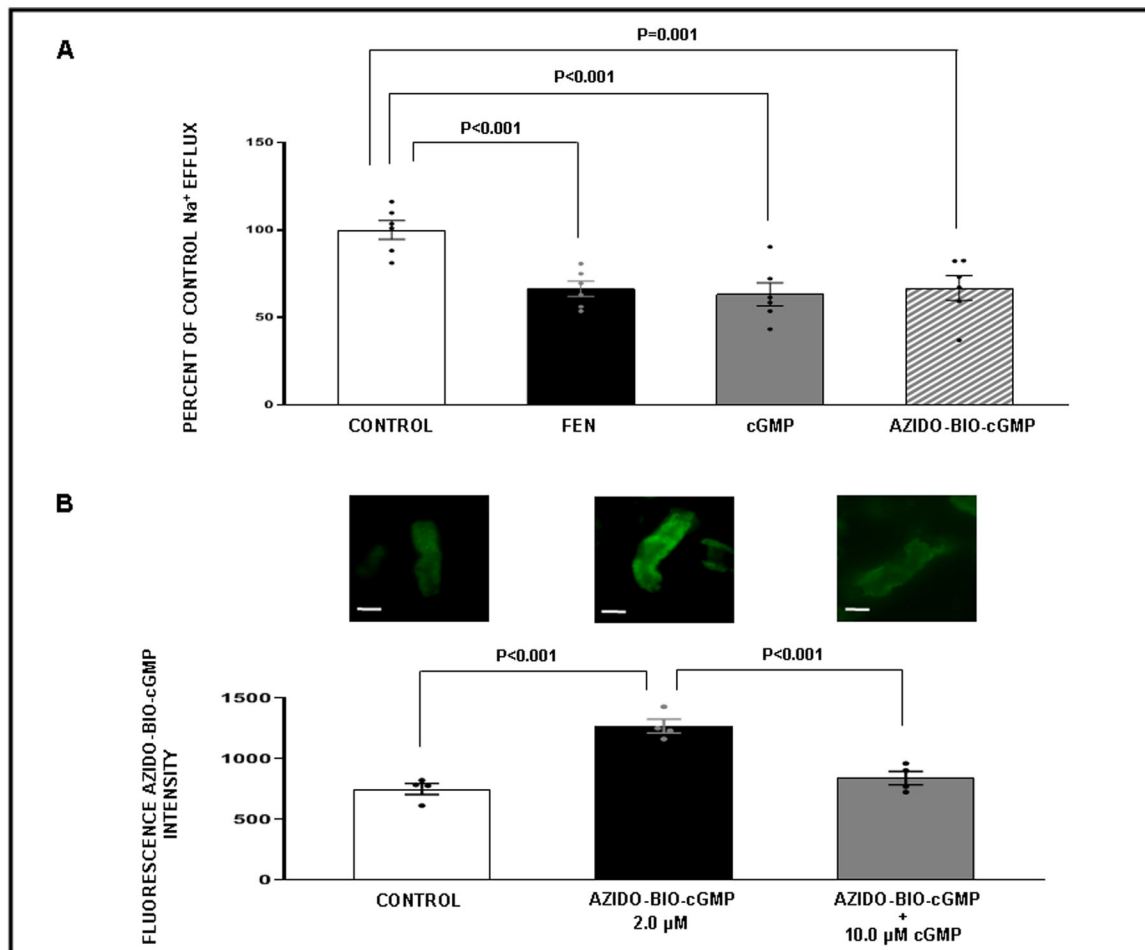


**Figure 3.**

**Panel A.** Sodium ( $\text{Na}^+$ ) efflux assay in WKY renal proximal tubule (RPT) cells in response to the following conditions. (□) Control: Opti-MEM. (■) Fenoldopam (FEN): 1  $\mu\text{M}$ . (▒) cGMP: 2  $\mu\text{M}$ . (▨) Azido-biotinylated-cGMP (Azido-BIO-cGMP): 2  $\mu\text{M}$ . For each condition measurements were taken from 6 separate wells in a 96-well plate with 20 locations measured per well. Results are presented as a percent of control  $\text{Na}^+$  efflux. **Panel B.** Competitive binding confocal microscopy experiments with RPTs isolated from normal rats ( $N=4$  for each experiment). The experiment was repeated 4 separate times using new fresh kidneys every time. Within each experiment, for each condition, measurements from 3 separate wells in a 96-well plate were averaged. Effects of cGMP on Azido-BIO-cGMP binding. (□) Control: Opti-MEM. (■) Azido-BIO-cGMP: 2  $\mu\text{M}$ . (▒) Azido-BIO-cGMP + cGMP: (10  $\mu\text{M}$ ). Control fluorescence values represent background. All other results are reported as Azido-BIO-cGMP fluorescence intensity above background. Data represent mean  $\pm$  1 SE. Scale bars represent 10  $\mu\text{m}$ . Statistical significance was determined by using the repeated measures analysis with an unstructured covariance matrix in SAS PROC MIXED program. The ANOVA with permutation P value was based on 2,000 permutations of group assignment to individual N values and a repeated measures analysis with an unstructured covariance matrix.

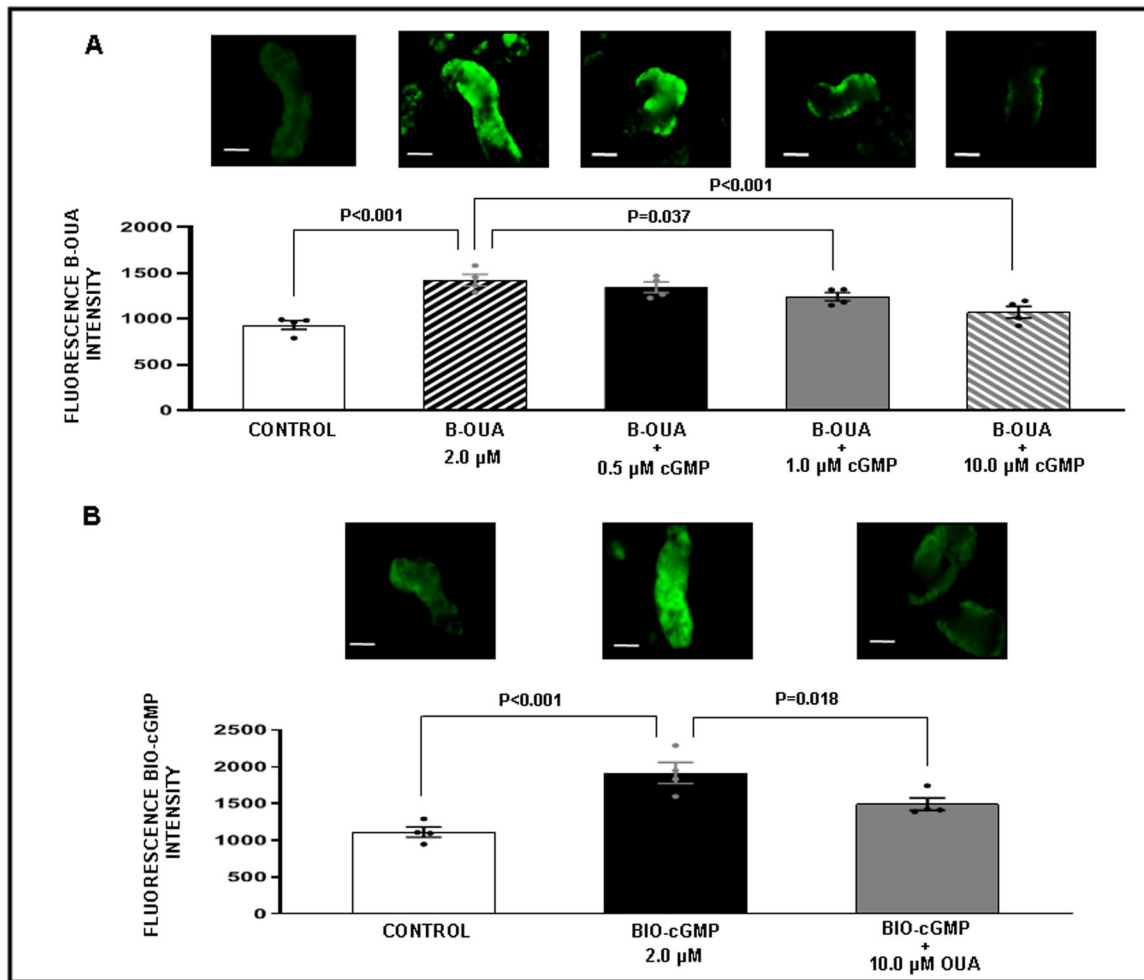


**Figure 4.**

Competitive binding confocal microscopy experiments with renal proximal tubules (RPT) isolated from normal rats (N=4 for each experiment). The experiment was repeated 4 separate times using new fresh kidneys every time. For each experiment and each condition measurements from 3 separate wells in a 96-well plate were averaged. **Panel A.** Effects of cGMP binding on bodipy-ouabain (B-OUA) binding. (□) Control: Opti-MEM. (▨) B-OUA: 2 μM. (■) B-OUA + cGMP: (0.5 μM). (▩) B-OUA + cGMP (1.0 μM). (▧) B-OUA + cGMP (10 μM). Control fluorescence values represent background. All other results are reported as B-OUA fluorescence intensity above background. **Panel B.** Effects of OUA binding biotinylated cGMP (BIO-cGMP). (□) Control: Opti-MEM. (■) BIO-cGMP: 2 μM. (▩) BIO-cGMP + OUA (10 μM). Control fluorescence values represent background. All other results are reported as BIO-cGMP fluorescence intensity above background. Data represent mean ± 1 SE. Scale bars represent 10 μm. Statistical significance was determined by using the repeated measures analysis with an unstructured covariance matrix in SAS PROC MIXED program. The ANOVA with permutation P value was based on 2,000 permutations of group assignment to individual N values and a repeated measures analysis with an unstructured covariance matrix.

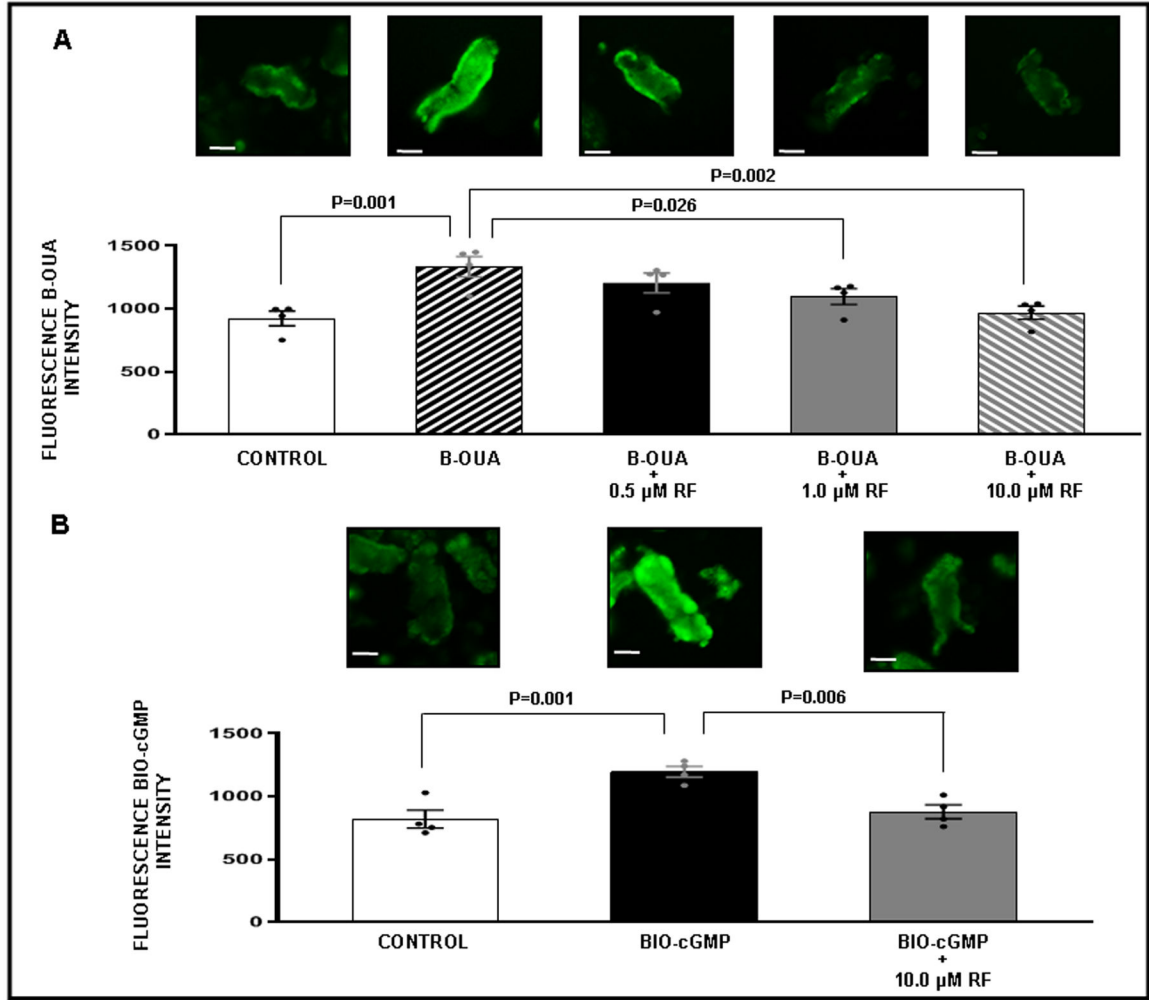


**Figure 5.**

Competitive binding confocal microscopy experiments with renal proximal tubules (RPT) isolated from normal rats (N=4 for each experiment). The experiment was repeated 4 separate times with new fresh kidneys. Within each experiment, each condition is represented by an average of 3 separate wells in a 96-well plate. **Panel A.** Effects of rostafuloxin (RF) binding on bodipy-ouabain (B-OUA) binding. (□) Control: Opti-MEM. (▨) B-OUA: 2 μM. (■) B-OUA + RF (0.5 μM). (▩) B-OUA + RF (1.0 μM). (▧) B-OUA + RF (10 μM). Control fluorescence values represent background. All other results are reported as B-OUA fluorescence intensity above background. **Panel B.** Effects of RF binding on biotinylated cGMP (BIO-cGMP). (□) Control: Opti-MEM. (■) BIO-cGMP: 2 μM. (▩) BIO-cGMP + RF (10 μM). Control fluorescence values represent background. All other results are reported as BIO-cGMP fluorescence intensity above background. Data represent mean ± 1 SE. Scale bars represent 10 μm. Statistical significance was determined by using the repeated measures analysis with an unstructured covariance matrix in SAS PROC MIXED program. The ANOVA with permutation P value was based on 2,000 permutations of group assignment to individual N values and a repeated measures analysis with an unstructured covariance matrix.



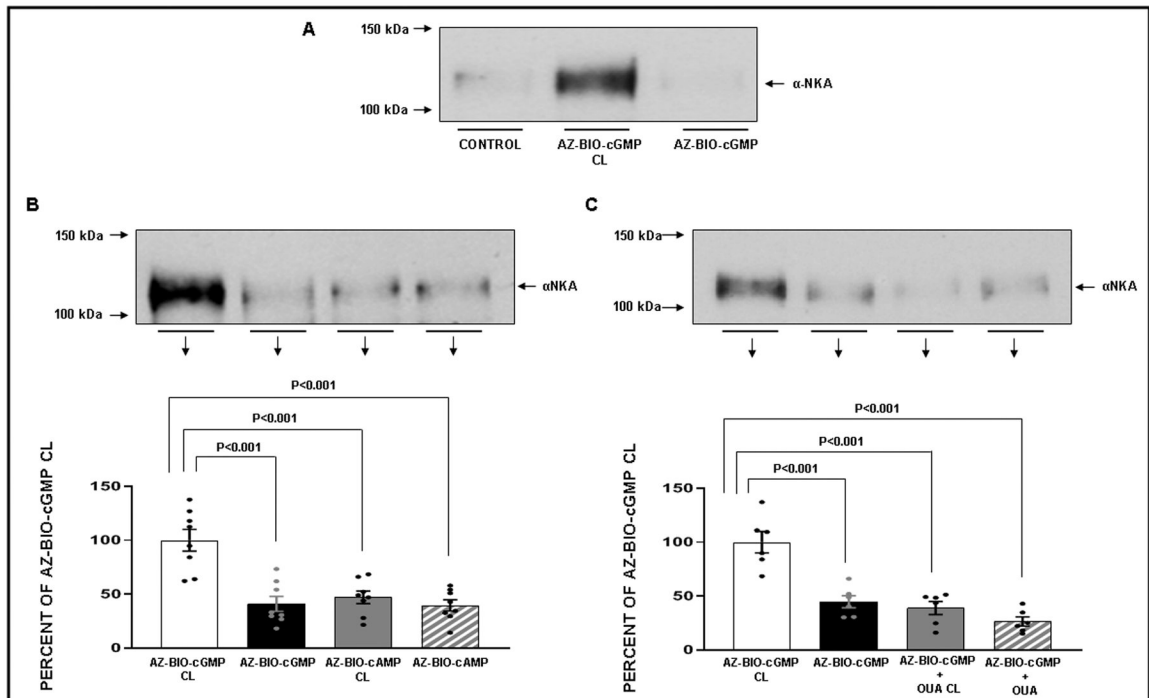


**Figure 6.**

**Panel A.** Effects of cross-linking (CL) of azido-biotinylated-cGMP (azido-BIO-cGMP) in isolated renal proximal tubules (RPT) from normal rats on  $\alpha$ NKA protein recovery in streptavidin adsorbates. The experiment was repeated 3 separate times with new fresh kidneys for each condition measured (N=3). (1) Control: Opti-MEM. (2) Azido-BIO-cGMP CL: 2  $\mu$ M. (3) Azido-BIO-cGMP Non-CL: 2  $\mu$ M. **Panel B.** Effects of CL of azido-BIO-cGMP and azido-biotinylated-cAMP (azido-BIO-cAMP) on  $\alpha$ NKA protein recovery. The experiment was repeated 8 separate times using new fresh kidneys every time (N=8). (□) Azido-BIO-cGMP CL: 2  $\mu$ M. (■) Azido-BIO-cGMP Non-CL: 2  $\mu$ M. (▨) Azido-BIO-cAMP CL: 2  $\mu$ M. (▩) azido-BIO-cAMP Non-CL: 2  $\mu$ M. Results are reported as percentages of azido-BIO-cGMP CL. **Panel C.** Effects of ouabain (OUA) on CL of azido-BIO-cGMP in isolated RPTs on  $\alpha$ NKA protein recovery. The experiment was repeated 6 separate times using new fresh kidneys every time for each condition measured (N=6). (□) Azido-BIO-cGMP CL: 2  $\mu$ M. (■) Azido-BIO-cGMP Non-CL: 2  $\mu$ M. (▨) azido-BIO-cAMP CL + OUA: 10  $\mu$ M. (▩) azido-BIO-cGMP + OUA Non-CL: 10  $\mu$ M. Results are reported as percentages of Azido-BIO-cGMP CL. Data represent mean  $\pm$  1 SE. Statistical significance was determined by using the repeated measures analysis with an unstructured covariance matrix in SAS PROC MIXED program. The ANOVA with permutation P value was based on 2,000 permutations of group assignment to individual N values and a repeated measures analysis with an unstructured covariance matrix.

MGKGVGRDKYEPAAVSEHGDKKSKKAKKERDMDDELKKEVSMDDHKLSLDELHRKYGTDLSRGLTPARAAEILARDGPNALTPPPTPEWVK  
 FCRQLFGGFSMLLWIGAILCFLAYGIRSATEEEPPNDLYLGVVLSAVVIITGCFSYQEAQSSKIMESFKNMVPPQALVIRNGEKMSINA  
EDVVVGDLEVEVGGDRIPADLRISANGCKVDNSSLTGESEPQTRSPDFTNENPLETRNIAFFSTNCVEGTARGIVVYTGDRVMGRIATL  
 ASGLEGGQTPIAEEIEHFHILITGVAVFLGVFFILSLILEYTWLEAVIFLIGIVANVPEGLLATVTVCLTLTAKRMARKNCLVKNLEAV  
ETLGSTSTICSDKTGTLTQNRMTVAHMMWFDNQIHEADTTENQSGVSFDKTSATWFALSRIAGLCNRAVFQANQENLPILKRAVAGDASESA  
LLKCIEVCCGSVMEMREKYTKIVEIPFNSTNKYQLSIHKPNASEPKHLLVMKGAPERILDRCSSILLHGKEQPLDEELKDAFQNAYLELG  
GLGERVLGFCHLLLPDEQFPEGFQFDTDEVNFPVDNLCFVGLISMIDPPRAAVPAVGVKCRSAGIKVIMVTGDHPITAKAIKGVGISEG  
NETVEDIAARLNIPVNVNPRDAKACVVHGSCLKDMTSEELDDILRYHTEIVFARTTSPQQKLIIVEGCQRQGAIVAVTGDGVNDSPALKKA  
DIGVAMGIVGSDVSKQAADMILLDDNFASIVTGVEEGRLIFDNLKKSIAYTLTLSNIPEITPFLIFIANIPLPLGTVTILCIDLGTDMVPA  
 ISLAYEQAESDIMKRQPRNPKTDKLVNERLISMAYGQIGMIQALGGFFTYFVILAENGLPFHLLGIRETWDDRWINDVEDSYGQQWYEQ  
 RKIVEFTCHTAFFVSIWVQWADLVICKTRRNSVFQQGMKNKILIFGLFEETALAAFLSYCPGMGAALRMYPLKPTWWFCAPYSLIFVY  
 DEVRKLIIRRPGGWVEKETYY

**Figure 7.**

Mass spectrometry peptide analysis of a cross-linked (CL) azido-biotinylated-cGMP (Azido-BIO-cGMP) sample. The sample was separated in a 10% Tris-HCL gel, stained with Coomassie SimplyBlue SafeStain, and a gel slice corresponding to molecular size of NKA (approx. 110 kDa) was excised and processed for mass spectrometry. The underlined red bold sequences indicate tryptic peptides identified by mass spectrometry when searched against the NCBI *Rattus Norvegicus* reference sequence using Byonic by Protein Metrics. Peptides were accepted with a false discovery rate of 1%. We identified 47 unique peptides covering 46.1% of the NKA amino acid sequence (472/1023 residues).

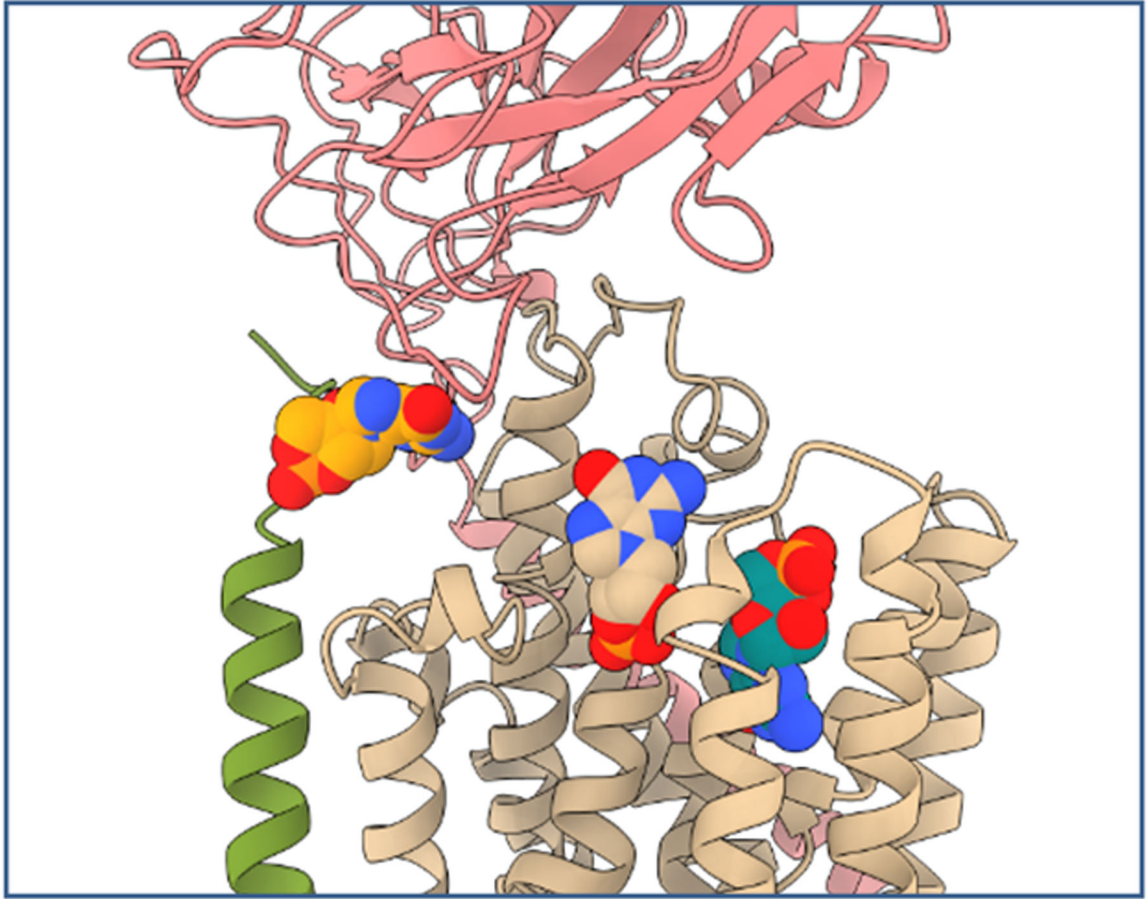


**Figure 8.** Docking of cGMP to NKA in the high affinity ouabain conformation. Three principle docking positions of cGMP to the extracellular site of NKA are shown. cGMP is depicted as spheres with the highest scoring model in tan, followed by teal and orange colored models. Porcine NKA subunits  $\alpha 1$ ,  $\beta 1$  and FXVD2 are shown as cartoon representations in tan, green and rose, respectively (PDB ID code 4HYT<sup>41</sup>).